A liquid helium target system for a measurement of parity violation in neutron spin rotation

C. D. Bass[*,a,b], T. D. Bass[b], B. R. Heckel[c], C. R. Huffer[a], P. R. Huffman[d], D. Luo[a], D. M. Markoff[e], A. M. Micherdzinska[a], W. M. Snow[a], H. E. Swanson[c], S. C. Walbridge[a]

[a]*Indiana University/IUCF, Bloomington, IN 47408, USA*
[b]*National Institute of Standards and Technology, Gaithersburg, MD 20899, USA*
[c]*University of Washington/CENPA, Seattle, WA 98195, USA*
[d]*North Carolina State University / TUNL, Raleigh, NC 27695, USA*
[e]*North Carolina Central University, Durham, NC 27707, USA*

Abstract

A liquid helium target system was designed and built to perform a precision measurement of the parity-violating neutron spin rotation in helium due to nucleon-nucleon weak interaction. The measurement employed an orthogonally-crossed neutron polarizer/analyzer pair surrounding the liquid helium target system. The expected parity-violating spin rotation of order 10^{-6} rad placed severe constraints on the target design. In particular, isolation of the parity-odd component of the spin rotation from a much larger background rotation caused by magnetic fields required a nonmagnetic cryostat and target system supported inside magnetic shielding, which allowed nonmagnetic motion of liquid helium between separated target chambers. This paper provides a detailed description of the design, function, and performance of the liquid helium target system.

Key words: Parity-violation, Neutron physics, Nucleon-nucleon weak interaction, Liquid helium, Polarized neutrons, Neutron optics, Cryogenic targets
PACS:

1. Introduction

The Neutron Spin Rotation experiment was proposed to measure the parity-violating spin rotation angle ϕ_{PV} of cold neutrons that propagate through liquid helium to a precision of 3×10^{-7} rad/m. The liquid helium target system for this experiment was assembled and tested at the Indiana University Cyclotron Facility (IUCF) in Bloomington, Indiana, and the experiment was conducted at the National Institute of Standards and Technology (NIST) in Gaithersburg, Maryland.

This paper describes the design, commissioning and performance of the liquid helium target system used in the Neutron Spin Rotation experiment. Section 1 provides a description of the phenomenon of parity-violation in neutron spin rotation and briefly discusses the scientific interest in its measurement, explains the design of the neutron polarimeter and the measurement strategy for isolating the parity-odd component of the neutron spin rotation, and describes the overall experimental apparatus, listing the requirements and constraints on the design of the liquid helium target. Section 2 specifies the design and construction of the liquid helium target system. Section 3 outlines the motion control system that was used to move liquid within the target. Section 4 describes the nonmagnetic cryostat and the cryogenic performance of the target system. Section 5 specifies the integration of the liquid helium target system into the data acquisition system. Section 6 provides details of the performance of the target, and Section 7 offers conclusions.

1.1. Physics Overview

From an optical viewpoint [1], neutron spin rotation is caused by the presence of a helicity-

*Corresponding author
Email address: christopher.bass@nist.gov (C. D. Bass)

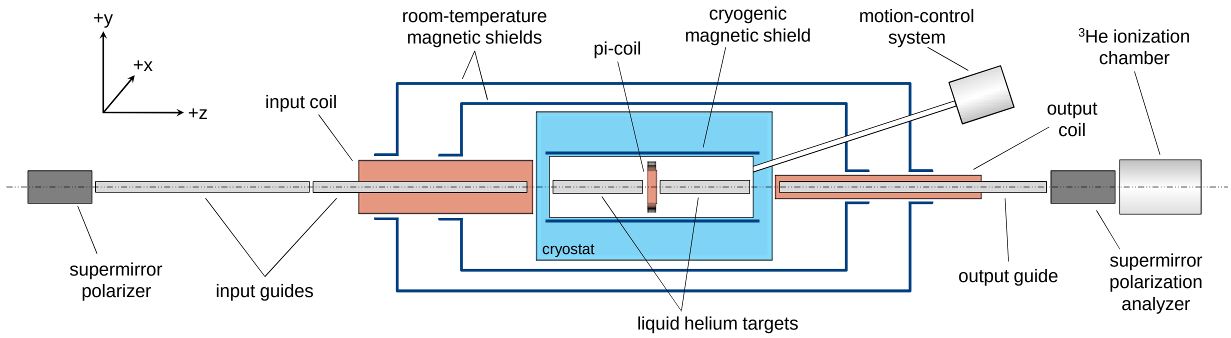

Figure 1: Schematic diagram of the neutron polarimeter apparatus for the Neutron Spin Rotation experiment.

dependent neutron index of refraction n of a medium, which can be given in terms of the coherent forward scattering amplitude $f(0)$ for a low-energy neutron:

$$n = 1 - \frac{2\pi\rho f(0)}{k^2}, \tag{1}$$

where ρ is the number density of scatterers in the medium, and $\vec{k}$ is the incident neutron wave vector. For low-energy (meV) neutrons propagating through an unpolarized medium, $f(0)$ is the sum of an isotropic, parity-even term f_{PC} that is dominated by the strong interaction and a parity-odd term f_{PV} that contains only weak interactions and is dominated by p-wave contributions. The f_{PV} term is proportional to $\vec{\sigma_{\mathrm{n}}} \cdot \vec{k}$, where $\vec{\sigma_{\mathrm{n}}}$ is the neutron spin vector, so f_{PV} has opposite signs for the positive and negative helicity neutron spin states.

As a neutron propagates through a medium, the two helicity states accumulate different phases: $\phi_{\pm} = \phi_{\mathrm{PC}} \pm \phi_{\mathrm{PV}}$. The parity-odd component causes a relative phase shift of the two neutron helicity components, and so induces a rotation of the neutron polarization about its momentum. Because the parity-odd amplitude is proportional to k, the rotary power per unit length $d\phi/dz = 4\pi\rho f_{\mathrm{PV}}/k$ tends to a constant for low-energy neutrons [2]. An order-of-magnitude estimate leads one to expect weak rotary powers in the $10^{-6} - 10^{-7}$ rad/m range.

Parity-violating neutron spin rotation is due to the nucleon-nucleon (NN) weak interaction and can be described in terms of the DDH nucleon-meson weak coupling amplitudes [3] as well as the pionless chiral EFT coupling parameters [4][5][6][7]. The values of these couplings are not well-constrained by theory, so a measurement of the parity-violating neutron spin rotation through liquid helium can constrain the poorly-understood properties of the NN weak interaction.

1.2. Measurement Technique

An overview of the neutron polarimeter is shown in Figure 1. The measurement technique – analogous to an arrangement of an orthogonally-crossed polarizer–analyzer pair in light optics – focuses on the orientation of the neutron polarization, which emerges along the $+\hat{y}$-direction from the supermirror polarizer.

In the absence of spin rotation, this orientation would remain unchanged during passage along the spin transport and into the target region. After leaving the target region, neutrons would enter the output coil, which transversely and adiabatically rotates the neutron polarization vector by $\pm\pi/2$ rad (see Figure 2). Neutrons would then pass through the polarization analyzer. Because the transmitted beam intensity for both $+\pi/2$ and $-\pi/2$ rotational states is the same, the difference in count rates measured by the ^{3}He ionization chamber would be zero.

However, if the neutron polarization rotates during beam passage through the target region, there would be a component of neutron polarization along the $\hat{x}$-direction (horizontal) when the beam reaches the output coil. This component would flip between the $+\hat{y}$ and $-\hat{y}$-directions as the output coil alternates between $+\pi/2$ and $-\pi/2$ rotational states. The transmission of neutrons polarized parallel to the axis of the polarization analyzer would be different than those polarized antiparallel, and this would produce an asymmetry in the count rates for the two output coil rotational states. The neutron

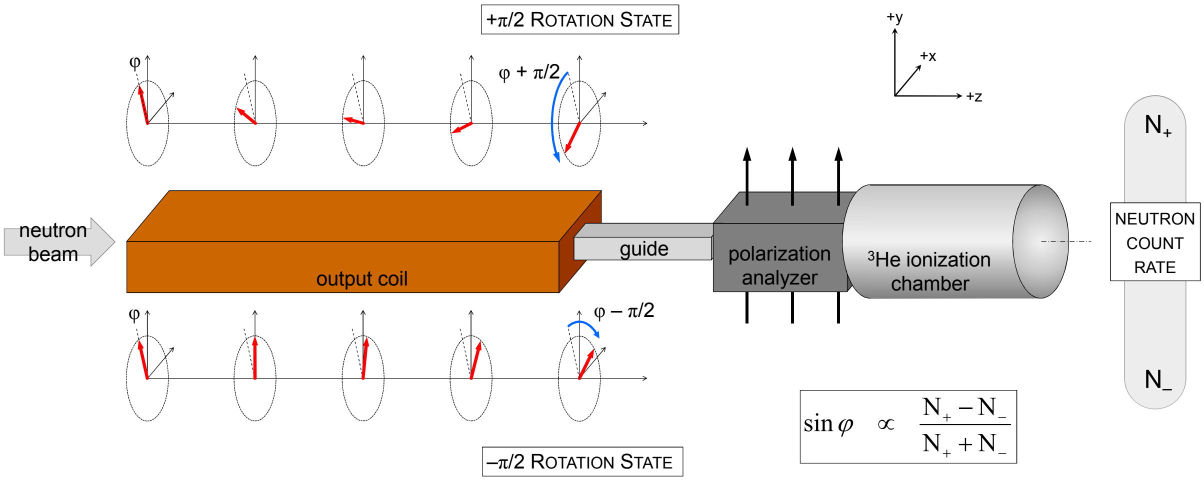

$$\sin\varphi \propto \frac{N_+ - N_-}{N_+ + N_-}$$

Figure 2: Diagram of the transverse rotation of neutron polarization by the output coil. The amount of spin rotation experienced by the neutrons along the target region is proportional to the count rate asymmetry measured in the ^{3}He ionization chamber between the two output coil rotational states.

spin-rotation angle ϕ_{PV} would be proportional to this count rate asymmetry.

Because longitudinal magnetic fields generate neutron spin rotation, it was necessary to separate the parity-violating component of the signal from this parity-conserving background. This was accomplished by oscillating the parity-violating signal at a known frequency.

Flipping the direction of neutron polarization does not change neutron helicity and so cannot be used to modulate the parity-violating signal. Instead, the oscillation was created by a combination of target motion and a precession of the neutron polarization about a vertical axis. Liquid helium was moved between a pair of target chambers located upstream and downstream of a vertical solenoid called a "pi-coil". The spin rotation along the target region due to magnetic fields was unaffected by the presence of liquid helium in either upstream or downstream target chamber, provided that (1) the target was nonmagnetic and (2) the trajectories and energies of neutrons accepted by the polarization analyzer and ^{3}He ionization chamber were unchanged when liquid helium was moved between the target chambers.

The pi-coil generated an internal magnetic field whose magnitude was chosen to precess the neutron polarization direction by π radians about the $\hat{y}$-axis for neutrons of a given energy. This precession effectively reversed the sign of the $\hat{x}$-component of neutron spin for rotations that occurred upstream of the pi-coil. With the pi-coil energized, the parity-violating contribution to the neutron spin rotation for liquid helium in the two target chambers changed sign, and the difference in the total spin rotation angle between the two target states was $2\phi_{\mathrm{PV}}$.

1.3. Physics Driven Parameters

In order to reach a measurement sensitivity of 3×10^{-7} rad/m, the neutron polarimeter and liquid helium target system needed to satisfy certain requirements. For an asymmetry measurement like the parity-violating spin rotation angle in a medium without neutron depolarization (and in the absence of systematic effects), the ideal target thickness can be shown to be two mean free paths [8]. In liquid helium at 4.2 K, the mean free path for 0.5 nm neutrons is about 1 meter, and this path length increases to about 2 m for 0.7 nm neutrons.

Next, the neutron polarimeter needed to effectively isolate the parity-violating spin rotation signal from a much larger parity-conserving background. As described above, this required modulating the parity-violating signal at a known frequency independent of the parity-conserving background. The relevant frequency band for this experiment was around 1 Hz, which was the frequency that the neutron spin rotation angle was measured by modulating the helicity of the magnetic field in the neutron spin transport. The choice of this frequency was constrained by (1) how quickly the fields in the spin transport coils could be reversed and stabilized, and (2) the expected frequency dependence of the neutron beam intensity noise from the reactor.

Finally, since most sources of systematic uncertainties scale with the strength of the longitudinal magnetic field in the target region, suppression of these effects to below the 5×10^{-8} rad/m level required a longitudinal magnetic field of less than 10 nT in the target region.

1.4. Overall Design Considerations and Constraints

The neutron polarimeter employed a target system that moved liquid helium between a pair of target chambers located upstream and downstream of a vertical solenoid in order to generate beam count-rate asymmetries, which were used to determine spin rotation angles. The location of liquid helium in the target should generate the parity-violating signal and not affect the parity-conserving background signal. Movement of liquid helium between target chambers should change the sign of the parity-violating signal but not its magnitude, and it should be done non-magnetically.

The presence of liquid helium in either the upstream or downstream target chamber defined a "target state" of the liquid helium target. The length of time that the liquid helium target remained in a given target state was determined by the need to maximize the beam count-rate statistics while minimizing the length of time between the beginning of consecutive target states. These time parameters were related to the data acquisition dead-time and to possible systematic effects caused by time-dependent magnetic fields in the target region.

In order to reduce the cost of the polarimeter and liquid helium target system, the collaboration chose to reuse several components from a previous experimental apparatus used to search for spin rotation in helium [9]. These components included a non-magnetic, horizontal bore cryostat; a pair of coaxial room-temperature magnetic shields with endcaps; input and output guide coils for the polarimeter; and the pi-coil. The 100 cm long bore of the cryostat bound the overall length of the liquid helium target assembly, which included the targets and pi-coil, mechanical supports, a cylindrical vacuum vessel that housed the target assembly, and necessary vacuum hardware and electrical instrumentation feedthroughs. In order to optimize available space, target chamber lengths were set to 42 cm.

The transverse dimensions of the target were determined by the cross-sectional area of the neutron beam at the exit window of the supermirror polarizer that was used for the experiment, which was 4.5 cm tall by 5.5 cm wide. The dimensions inside the target chambers allowed maximum acceptance of the beam with sufficient space for internal collimation. Combined with the target length, these dimensions determined the target volume.

Finally, the need to suppress the magnetic field inside the target region severely affected the design of the liquid helium target system and the spin transport of the polarimeter. Within the target region, only non-magnetic and low-permeable materials were used – all hardware was checked explicitly for magnetic inclusions or impurities, and any item that produced changes in the ambient magnetic field of more than 1 nT when moved past a fluxgate magnetometer sensor at a distance of 1 cm was rejected.

The current-carrying wires of the pi-coil and the instrumentation generated undesired magnetic fields. Twisted-pair wires were used for all wiring within the target region in order to suppress associated magnetic fields. Furthermore, all instrumentation was powered off during data-taking and energized during target changes as required.

1.5. Experimental Layout

Low energy ($\sim 10^{-3}$ eV) neutrons from the NIST Center for Neutron Research (NCNR) cold source were transported to the end station of the NG-6 polychromatic beam line and passed through cryogenic blocks of bismuth and beryllium, which filtered out gamma rays and fast neutrons, and short wavelength cold-neutrons (respectively). Transmitted neutrons passed into the neutron polarimeter apparatus as shown in Figure 1.

At the upstream end of the apparatus, neutrons were vertically polarized in the "up" direction ($+\hat{y}$-axis) by a supermirror polarizer. They traveled along a 1.25 m long guide tube that was filled with helium gas and passed through an input coil, whose vertical field preserved the alignment of the beam polarization. Neutrons passed through a current sheet at the end of the input coil, and so the neutron spin was non-adiabatically transported into the magnetically shielded target region.

Reducing the ambient 50 mT field to less than 10 nT in the target region was accomplished using a combination of room-temperature and cryogenic mu-metal shielding. Transient fields in the NCNR guide hall generated by equipment and other experiments were suppressed by compensation coils that were mounted outside the room-temperature mu-metal shielding. Magnetometery located in the target region provided control feedback to the compensation coils.

After passing into the target region, neutrons were collimated into separate left and right sub-beams and allowed to enter the liquid helium target. Neutrons propagated through the target and then entered the output coil, which non-adiabatically guided the neutron spin out of the target region. The output coil also transversely rotated the neutron polarization vector by $\pm\pi/2$ rad. The sub-beams then passed through a supermirror polarization analyzer whose polarization axis was aligned with that of the supermirror polarizer. Transmitted neutrons then entered a ^{3}He ionization chamber operating in current mode and which generated a signal proportional to the neutron count rate. The asymmetry in the count rates measured after changing the helicity of the magnetic transport field in the output coil was proportional to the neutron spin rotation angle.

2. Liquid Helium Target

The liquid helium target consisted of a pair of vessels located upstream and downstream of the pi-coil. Each vessel was partitioned into separate left and right-side chamber pairs, which created four identical target chambers that could each hold liquid helium. This partitioning effectively created upstream and downstream chamber pairs along the left and right-side sub-beams and formed two parallel experiments when combined with the polarimeter design.

Each target chamber possessed an inlet and outlet for transferring liquid helium. Inlets from all four chambers were connected to a centrifugal pump that was immersed in a 13 L liquid helium bath located in the bottom of a cylindrical vessel called the vac-canister. By operating the centrifugal pump, all four target chambers could be filled with liquid helium.

Each outlet was connected to a flexible drainpipe that could be moved above or below the height of nominally full or empty (respectively) liquid helium levels inside the target chambers. By lowering a drain, a target chamber could be emptied of liquid helium and its contents returned to the bath. The volume of the bath in the bottom of the vac-canister was maintained by periodic transfer of liquid helium from an external dewar. Alternately filling and draining diagonal pairs of target chambers with liquid helium created the two target states that were necessary to extract the parity-violating spin rotation angle ϕ_{PV}.

2.1. Vac-canister

The vac-canister was a 95.3 cm long by 28.8 cm diameter cylindrical aluminum vacuum chamber that housed the liquid helium target. Upstream and downstream targets – as well as the pi-coil – were bolted to an aluminum support rail that mated into a set of matching rails in the bottom of the vac-canister. This rail system provided alignment of the target within the vac-canister.

Main flanges with indium o-ring seals were located on the upstream and downstream ends of the vac-canister. Both of the main flanges had a 0.8 mm thick aluminum flange with an indium o-ring seal covering a beam window. During leak checks and data taking operation, the vac-canister and beam windows were shown to withstand an internal pressure difference of 270 kPa and an external pressure difference of 101 kPa without leak or rupture of the windows at both room temperature and cryogenic temperatures. In addition, the downstream main flange was built to accept two custom-built nonmagnetic electrical feedthroughs [10], a motion-control feedthrough tube, and a liquid helium transfer tube, along with spare access ports. All seals used aluminum ConFlat[1](CF) flanges and gaskets or indium joints, and all metals were brass, aluminum or titanium. All components were thermally cycled several times in preliminary tests and later were shown to be superfluid leak tight in low temperature tests at IUCF.

Around the outside of the vac-canister, ten equally spaced coils connected to individual current supplies provided magnetic field compensation inside a layer of cryogenic magnetic shielding that lined the cold bore.

[1]Certain commercial equipment, instruments, or materials are identified in this paper in order to specify the experimental procedure adequately. Such identification is not intended to imply recommendation or endorsement by the National Institute of Standards and Technology, nor is it intended to imply that the materials or equipment identified are necessarily the best available for the purpose.

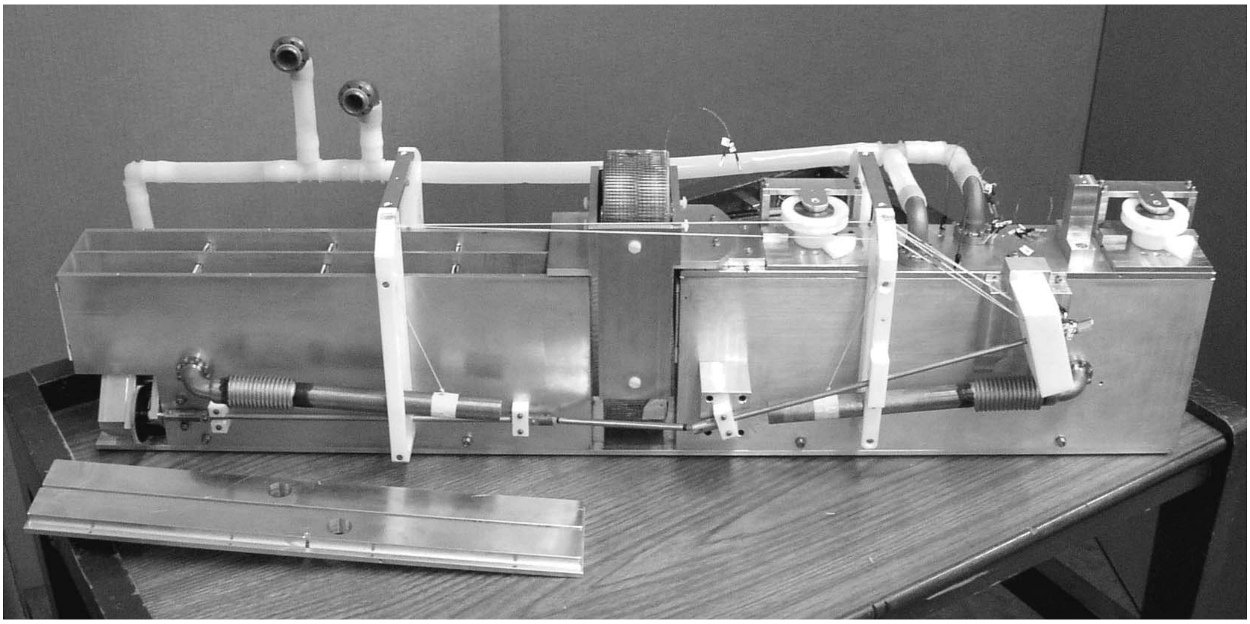

Figure 3: Photo of the liquid helium target showing the pump and drain system, the pi-coil, and instrumentation.

The vac-canister rested within this cryogenic magnetic shielding on four ceramic balls, which thermally isolated it from the rest of the cryostat. The vac-canister could slide along the cold bore due to differential thermal contraction of the motion-control feedthrough and liquid helium transfer tubes, which connected the vac-canister to the motion-control box located outside the target region. A pair of titanium bolts protruded through the cryostat upstream 4-K thermal shield and provided a low thermal conductivity mechanical stop for the upstream movement of vac-canister.

2.2. Target Chambers

The 420 mm long by 80 mm wide upstream and downstream targets were each machined from monolithic pieces of 6061 aluminum. Aluminum was chosen as the target chamber material since it is nonmagnetic, has a high thermal conductivity, and has a low neutron scattering and absorption cross section [11].

A wire electrical discharge machine (EDM) at the University of Washington was used to create left and right-side chambers in each target that were 416 mm long by 33.5 mm wide by 60 mm deep; the chambers were separated by a 3 mm thick septum that isolated the left and right sides (see Figure 3). Special care was taken to ensure that all surfaces exposed to the neutron beam were flat and normal to the mean beam direction to minimize possible systematic effects from neutron refraction. In addition, special care was taken to make the target dimensions, especially the target lengths, as identical as possible to minimize possible systematic effects. The measured length difference at room temperature between all four target chambers was less than 0.01 mm.

2.3. Neutron Beam Collimation

Because of beam divergence or small angle scattering, some neutrons could reflect from a target chamber wall and still be transmitted through the polarimeter and counted in the ^{3}He ionization chamber. The critical angle for neutron reflection between helium and aluminum depends on the difference in the neutron index of refraction of the two materials, which is proportional to density and therefore changes with the liquid or gas state of the helium. These differences can cause systematic effects through target-dependent neutron beam intensity and phase space changes coupled to residual magnetic fields in the target region. This subclass of neutron trajectories was prevented from reaching the ^{3}He ionization chamber by collimation of the beam.

Within each target chamber, a set of three ^{6}LiF-plastic collimators prevented neutrons from reflecting off the chamber walls and reaching the detector

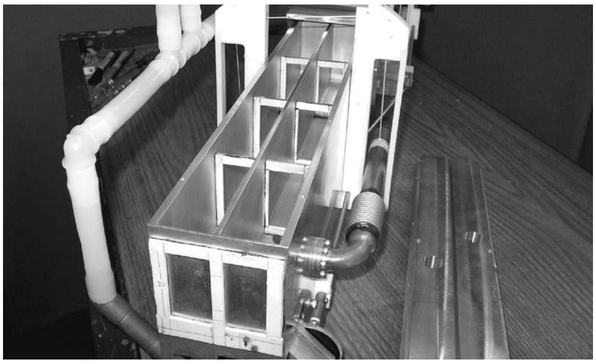

Figure 4: Layout of the neutron beam collimation within a target. ^{6}LiF-plastic was glued onto aluminum backing frames and then glued into the target chambers. The size and spacing of the collimation was chosen to prevent neutrons with wavelengths larger than 2 nm from reflecting off a chamber wall and then being accepted into the ^{3}He ionization chamber. Additional ^{6}LiF-plastic was glued onto the upstream face of the targets.

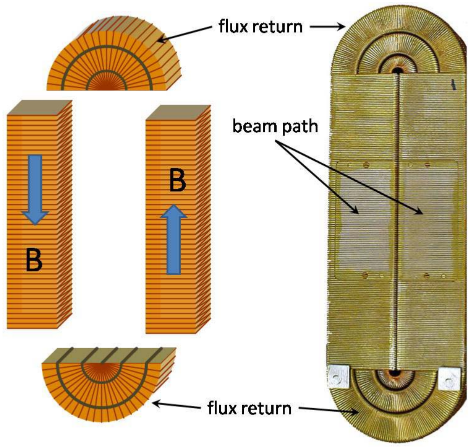

Figure 5: Diagram of the pi-coil. The coil is wound so that the left and right solenoids produce vertical magnetic fields through the region of the passing neutron beam. These fields are oriented opposite to each other, and the curved solenoid sections on top and bottom provide flux return for both coils.

as shown in Figure 4. Collimators were positioned at 1/4, 1/2, and 3/4 of the length of the target chambers. Collimators extended into the target chamber 5 mm along the top, bottom, and outer chamber walls, and 2 mm along the chamber septum. This collimation defined the sub-beam within a target chamber as 26.5 mm wide by 50 mm tall.

The incident neutron beam possesses a broad energy spectrum, which begins at the cold source as a Maxwellian distribution corresponding to a temperature of 40 K. Becuase the critical angle of the neutron optical mirrors which transport the neutrons to the apparatus increases with the neutron wavelength, any particular choice of collimation suppresses reflected neutrons only below some cutoff wavelength. The geometry and spacing of the collimators described above sufficed to prevent neutrons with wavelengths less than 2 nm from reflecting off target walls and being accepted by the ionization chamber. The neutron beam intensity for wavelengths above 2 nm in a long ($\sim$60 m) guide like that used at NCNR is typically over three orders of magnitude smaller than the higher energy portion of the beam. This fraction of the beam is too small to make a significant contribution to the systematic uncertainty in the measurement.

The collimators were built from ^{6}LiF-plastic that was glued to an aluminum backing with Stycast 2850FT epoxy resin and then glued into the target chambers. Additionally, ^{6}LiF-plastic was glued to the upstream face of each target and defined the left and right-side neutron sub-beams with the same collimation as those inside the target chambers.

2.4. Pi-Coil

The pi-coil generated an internal magnetic field that precessed the transverse component of neutron spin about the $\hat{y}$-direction. The amount of spin precession was determined by the strength of the magnetic field and the neutron velocity. The pi-coil was tuned to rotate the mean wavelength (approximately 0.5 nm) of the neutron beam by π rad.

The pi-coil was built from a pair of side-by-side, 40 mm square cross-section solenoids that were 160 mm tall (see Figure 5). A pair of curved solenoids provided flux return on the top and bottom of the pi-coil, and the currents in the two coils flowed in opposite directions so that the magnetic flux was contained within the coils to high accuracy. Each solenoid in the pi-coil was wound around an aluminum core with three layers of 28 gauge copper magnet wire at a winding density of 10 wires per cm per layer.

The pi-coil was fixed in place between the upstream and downstream target chambers by nylon set screws that were bolted into a surrounding aluminum mount. The screws pressed onto aluminum relief plates that were glued to the outside of the pi-coil in order to prevent windings from being dam-

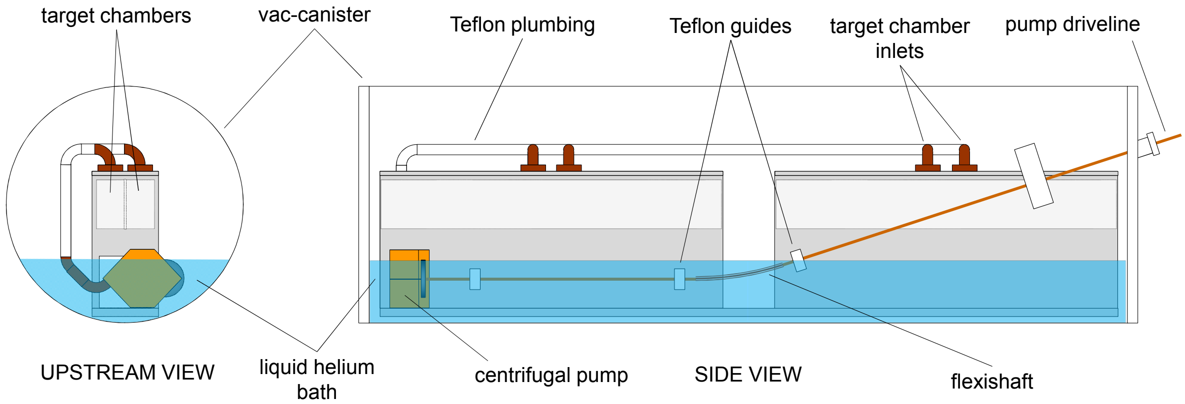

Figure 6: Schematic of the centrifugal pump system. A stepper motor positioned outside the target region provided torque to the centrifugal pump along a driveshaft in the motion-control feedthrough tube and a driveline in the vac-canister. The centrifugal pump moved liquid helium from a bath in the bottom of the vac-canister into plumbing that connected to the four target chamber inlets located in the target lids.

aged. The mount was attached to the upstream and downstream target chamber lids. A brass pin was fit into the bottom flux return of the pi-coil and coincided with its geometric vertical axis. The pin rested in a transverse groove in the target support rail, which also secured the target chambers.

The height of the support pin and the positions of the set screws were chosen to center the pi-coil in the beam as defined by the target chamber collimation. The geometric axis of the pi-coil was positioned to coincide with the vertical axis of the target as defined by the partition between target chambers. The pi-coil was positioned equidistant between the targets approximately 20 mm from the inside surface of the target chambers.

2.5. Centrifugal pump and drain system

Isolating the parity-violating component of the neutron spin rotation through target motion required a method of changing target states that filled and drained diagonal pairs of target chambers without changing the magnetic fields inside the target region. This was accomplished with a centrifugal pump that was immersed in a 13 L liquid helium bath located in the bottom of the vac-canister and a set of flexible drainpipes that were connected to outlets located at the bottom of each target chamber.

The centrifugal pump was similar in size and design to positive-displacement pumps that have previously been used to move both normal and superfluid helium [12]. The pump was tested thoroughly in liquid nitrogen at IUCF before operation at liquid helium temperature. The torque needed to spin the impeller was transferred from a stepper motor located outside of the target region through a carbon fiber driveshaft within the motion-control feedthrough tube and through a driveline inside the vac-canister that was built from brass rod and flexible copper braided-wire rope (Figure 6).

The volume throughput of the centrifugal pump was a function of impeller speed and the depth of the liquid helium bath. The maximum rotation frequency of the stepper motor feedthrough was 300 rev/min. The centrifugal pump had a 4:1 gear ratio, which set the maximum impeller rotational speed at 120 rev/min. In practice, operating the stepper motor above 120 rev/min caused the pump and driveline to seize. This rotation speed could fill all four target chambers with liquid helium in 250 s to 300 s, depending on the depth of the bath.

Target chambers were emptied of liquid helium by drainpipes that could be raised or lowered by braided polyester strings, which were routed through the target and motion-control feedthrough tube through Teflon and carbon fiber sleeves to a pair of pneumatic linear actuators located outside of the target region. Drainpipes from diagonal pairs of target chambers (e.g. upstream-right and downstream-left) were operated together from

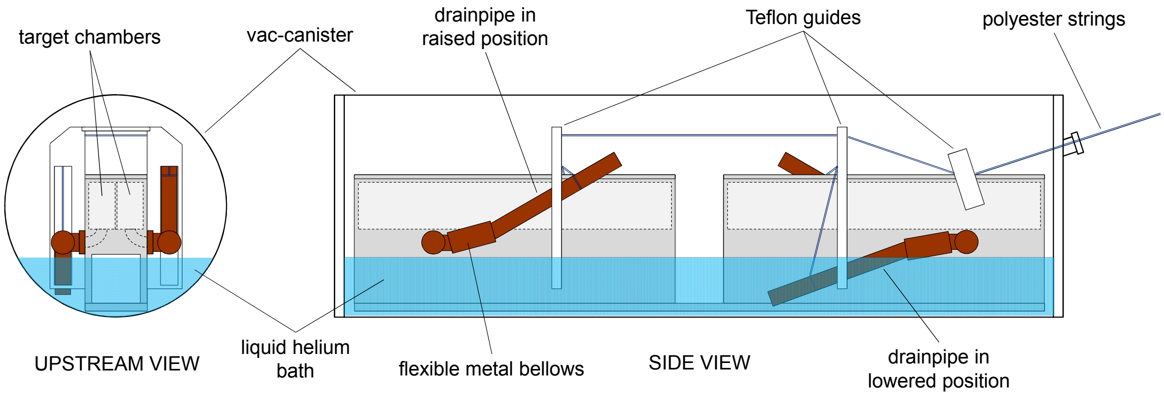

Figure 7: Schematic diagram of the drain system. Actuators located outside the target region move strings connected to the ends of drainpipes that are attached to the outlets of the target chambers via flexible metal bellows. The raised or lowered position for each drain was chosen to ensure that the tip of the drainpipe was above the full liquid level or below the empty level (respectively) for a target chamber.

a single actuator and could empty a target chamber of liquid helium in 50 s when lowered (Figure 7).

Inside each target chamber, square grooves were machined into the floor and lid to ensure that liquid helium or helium gas did not collect along the bottom or top (respectively) of the chambers between collimators, which would have created a helium liquid/gas interface, which might reflect some neutrons that would otherwise be stopped by the collimation and be counted in the ^{3}He ionization chamber.

2.6. Pyroelectric Ice Getters

The centrifugal pump had gears and other moving parts that could in principle be jammed by solid impurities mixed within the liquid helium. Possible impurities include ice crystals from water or liquid air accidentally introduced into the target system during a liquid helium transfer or from the ice slurry found in the bottom of a typical liquid helium research dewar. These impurities caused the gears of the pump to seize in the first version of the experiment. We decided to protect the centrifugal pump with a pyroelectric object.

Cesium nitrate is a ferroelectric that spontaneously polarizes at cryogenic temperatures [13] and remains polarized at constant temperature in a cryogenic environment. Cesium nitrate powder was mixed with urethane resin and cast into discs 75 mm in diameter by 5 mm thick. The discs were bolted onto the lower section of each target, so they would be immersed in the liquid helium bath.

Although we made no attempt to measure the impurities that may have been present in the liquid helium inside the target, based on our experience it is quite unrealistic to assume that they were absent. In our judgement, the most likely explanation for the fact that the same centrifugal pump used in the previous experiment did not seize over several months of nearly continuous operation is the presence of these getters.

3. Motion Control System

In order to change target states, liquid helium needed to be non-magnetically moved between target chambers. The liquid helium target system employed a pump and drain system that was operated outside of the target region by the motion-control system.

The motion-control system consisted of a stepper motor and driveshaft, which turned the centrifugal pump, and a pair of pneumatic linear actuators that were attached to the drains by strings. The stepper motor and actuators were connected to a vacuum chamber called the motion control box (MCB), which shared the same helium environment as the target system inside of the vac-canister (Figure 8). A motion-control feedthrough tube guided the driveshaft and actuator control strings from the

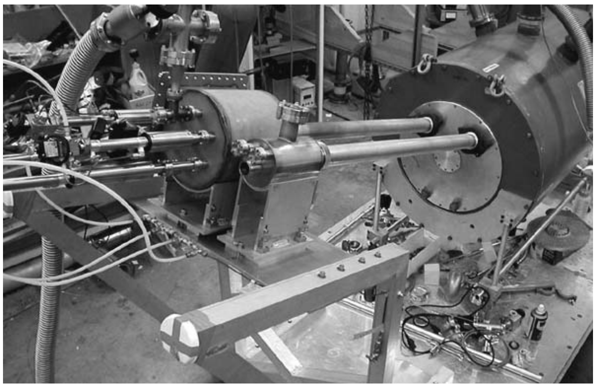

Figure 8: Photo of the motion-control system. The MCB (A) was positioned downstream of the cryostat and the magnetic shielding (not shown) and above the height of the beam line. Pneumatic linear actuators and a stepper motor attached to the downstream face of the MCB, while the motion-control feedthrough tube and its vacuum jacket connected into the upstream face of the MCB. Control strings and the driveshaft from the feedthrough tube were connected to the actuators and stepper motor inside the MCB, which were accessible by a demountable acrylic window. The vacuum-jacketed liquid helium transfer line connected to a valve assembly (B), which allowed the use of an external dewar to periodically refill the target bath.

MCB into the vac-canister through penetrations in the magnetic shielding and cryostat.

The motion-control feedthrough tube was constructed from thin-walled G10-grade glass epoxy laminate tube, which was coated with epoxy resin and surrounded by a layer of reflective aluminum tape. The epoxy resin provided additional mechanical stiffness to the laminate tube and suppressed helium diffusion and light transmission through the wall of the laminate. The aluminum tape provided a highly reflective surface that suppressed radiative heat transfer by thermal radiation from the aluminum vacuum jacket that surrounded the motion-control feedthrough tube. An aluminum CF flange was glued into the cold end of the tube, and a 316 stainless steel bellows assembly was glued into the room temperature end, which was located outside of target region (Figure 9).

A guide assembly was housed within the length of the motion-control feedthrough tube and was built from four small diameter carbon fiber tubes that were glued into a set of baffles. The carbon fiber tubes sheathed the braided polyester control strings that connected the target chamber drains to actuators within the MCB. The baffles provided mechanical support to the carbon fiber tubes and allowed the guide assembly to slide within the motion-control feedthrough tube under differential thermal contraction. The baffles also prevented light and thermal radiation from shining onto the interior of the vac-canister and segmented the helium gas column within the motion-control feedthrough tube to suppress potential heat loads due to gas convection. A drilled hole in each baffle supported and aligned the carbon fiber driveshaft, which connected the centrifugal pump driveline in the vac-canister to the stepper motor located in the MCB. Teflon caps were inserted into each end of the motion-control feedthrough tube and provided a smooth bearing surface for strings and driveshaft.

The driveshaft coupled to the stepper motor inside the MCB via a stainless steel double universal joint. The control strings attached onto the ends of actuators through brass tension springs. The lengths of the strings were chosen to ensure that each drain would travel through its entire range of movement, and the springs provided tension relief for the strings. The springs were chosen so that they would mechanically fail before a string broke in case of a stuck string. The MCB possessed a large access port with a Buna-N o-ring seal and a acrylic window for both visual inspection and (if needed) mechanical repair of the springs, strings and actuators.

The aluminum vacuum jacket that surrounded the motion-control feedthrough tube coupled into the MCB through a fluorosilicone compression o-ring seal. This type of material remains plastic through a wider temperature range than typical silicone or fluorocarbon o-rings, which was important since the MCB became cold during target operation. During liquid helium transfers or other periods of rapid cryogenic liquid boil-off in the target, heater tape was used to guard against the development of vacuum leaks due to o-ring embrittlement caused by excessive cold.

4. Cryogenics

4.1. Cryostat

A horizontal bore, nonmagnetic cryostat was originally built by Oxford Instruments for a previous experiment to measure parity-violating neutron spin rotation in liquid helium. All of the vacuum joints that were originally glued had failed, and so new joints were redesigned and replaced with either soldered or indium-sealed joints as applicable.

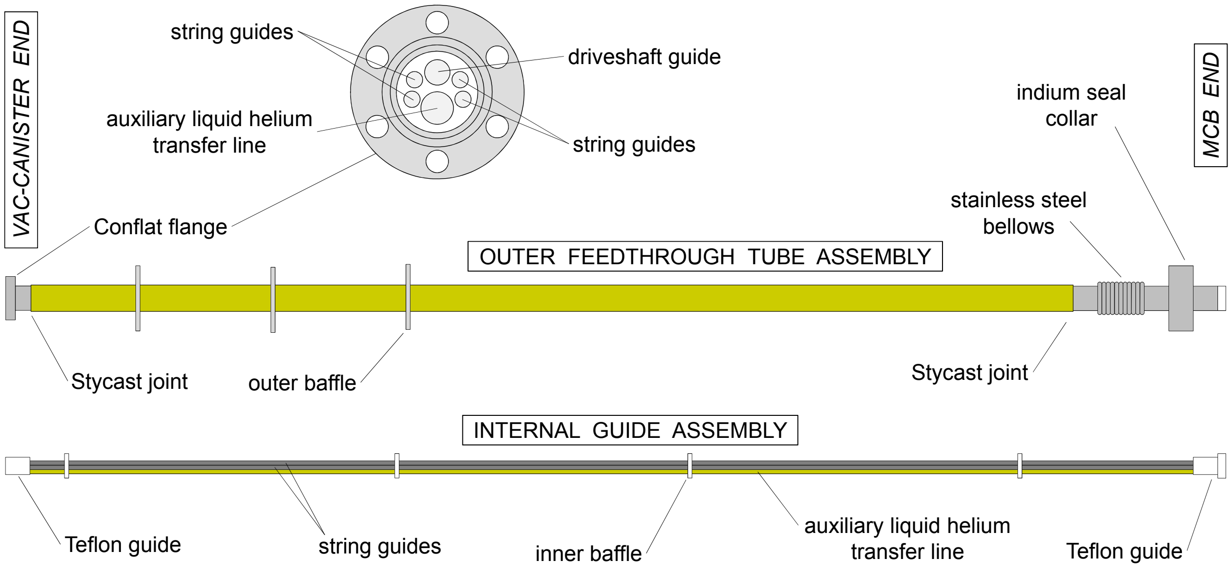

Figure 9: Schematic diagram of the motion control feedthrough tube. Four carbon fiber tubes that sheathed the drainpipe strings were glued into a set of thermal radiation baffles. A hole in each baffle guided the pump driveshaft. The bundle fit within a laminate tube and was capped by Teflon guides on each end. The laminate tube was externally coated with a layer of epoxy resin and reflective aluminum tape. A set of baffles were glued on the outside of the laminate tube to suppress radiative heat loads on the vac-canister. An aluminum CF flange and a stainless steel bellows assembly were glued into the ends of the feedthrough tube.

The cryostat consisted of two coaxial annular aluminum vessels housed within an aluminum cylindrical main vacuum vessel as shown in Figure 10. The outer 77-K vessel could hold 50 L of liquid nitrogen, and the inner 4-K vessel could hold 30 L of liquid helium. The measured hold time of the cryostat during nominal data runs was 50 h for liquid nitrogen and 30 h for liquid helium, which allowed a convenient daily refill schedule.

The cylindrical interior surface of the 4-K vessel formed the cold bore, which was 305 mm in diameter by 1000 mm long. A cryogenic magnetic shield built from Amuneal Cryoperm 10 lined the cold bore. Cryoperm 10 was chosen because its permeability at cryogenic temperatures is comparable to that of normal mu-metal at room temperature.

All materials of the cryostat that were located inside the room-temperature magnetic shielding were nonmagnetic. The two annular vessels were independently suspended within the main vacuum vessel by adjustable G-10 straps and braces for thermal isolation and adjustability. The cryostat was supported within the magnetic shielding by a set of four aluminum posts, which passed through small openings in the shielding. The posts fit inside machined inserts and supported the cryostat from its ends.

4.2. Liquid Helium Transfer Tube

The liquid helium target was subject to a heat load that boiled away the liquid helium in the vac-canister, which decreased the depth of the liquid helium bath over time. A minimum bath depth was required for changing target states, so the vac-canister was periodically refilled from an external dewar through a liquid helium transfer tube that entered the vac-canister through an external valve and compression o-ring fitting assembly located outside of the target region and magnetic shielding.

The liquid helium transfer tube was of similar design as the motion-control feedthrough tube (see section 3), except that there was no internal guide assembly. An aluminum vacuum jacket surrounded the liquid helium transfer tube.

4.3. Heat Load

The boil-off rate of liquid helium in the vac-canister determined the upper bound on the length of a data run. Suppressing this heat load allowed longer data runs and therefore greater statistical accuracy for the spin rotation measurement. Considerable effort was therefore devoted to the reduction of possible heat leaks in the system. The challenge was to achieve low heat leaks in a liquid helium target system which necessarily possesses direct mechanical linkages between room temperature and the inside regions of the vac-canister.

The liquid helium target system was designed and operated to minimize the heat load on the vac-canister and target. Electrical instrumentation in the target was turned off when not required in order to reduce the heat load generated by current-carrying wires and sensors. This included turning off the pi-coil during target changes.

All cryogenic surfaces were either polished or layered with reflective aluminum tape or superinsulation to suppress radiative heat transfer. Aluminum heat shields were bolted onto the upstream and downstream annular faces of the cryostat liquid helium vessel, which provided nearly 4π coverage of the vac-canister surface with a 4 K surface. A second set of heat shields anchored to the cryostat liquid nitrogen vessel provided a 77 K surface exterior to the 4 K surface. Beam windows on these heat shields were covered with aluminum foil, and the inner face of each shield was covered with cryogenic super-insulation.

Both the motion-control feedthrough tube and the liquid helium transfer tube penetrated the 4-K and 77-K heat shields and were sheathed by a pair of aluminum vacuum jackets outside of the target region. The outer surface of these tubes were wrapped with super-insulation, and each of them employed a set of exterior baffles that suppress 300 K thermal radiation from being incident on the vac-canister through openings in the heat shields.

All components anchored to a surface warmer than 4 K were constructed using materials that possessed low thermal conductivity and were sufficiently long to suppress conductive heat transfer. The wiring harness for the target instrumentation was thermally lagged to the heat shields. Similarly, the motion-control feedthrough tube and the liquid helium transfer tube were thermally lagged to the downstream 4-K and 77-K heat shields with braided copper straps.

The design estimate for the total heat load on the liquid helium target was 100 mW to 150 mW. However, this estimate was too small to explain the observed bath boil-off rate of about 10 L of liquid helium every 6 h to 8 h. A numerical simulation

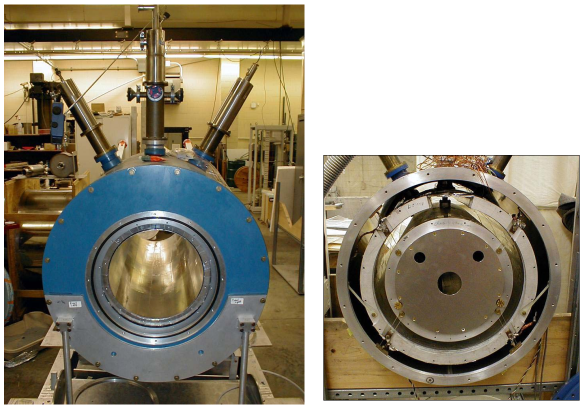

Figure 10: Photos of the cryostat. The outer 77-K vessel held liquid nitrogen and the inner 4-K vessel held liquid helium. The inside diameter of the 4-K vessel formed the cold bore and was lined with cryogenic mumetal magnetic shielding.

was conducted of the thermal transport along the motion control feedthrough tube and the liquid helium transfer tube, which revealed that the layer of reflective aluminum tape wrapped around the outer surface of each tube conducted 140 mW to 225 mW from the MCB and liquid helium valve transfer port at room-temperature to the vac-canister at 4 K. Including the effects of the radiative heat load along the length of each tube from the surrounding room-temperature vacuum jackets – which was what the aluminum tape was introduced to suppress – added another 20 mW.

In addition, the simulation indicated that the heat load along the tubes due to the 77-K thermal lagging straps was substantial, since the copper braids mechanically coupled onto each tube about 20 cm from the face of the vac-canister. The straps were anchored to the 77-K heat shield, which could be tens of degrees warmer than the cryostat 77-K vessel to which it was coupled. The 4-K thermal lagging straps, which connected onto the tubes about 10 cm from the vac-canister, partially offset the heat load due to the 77-K straps. But, the 4-K straps were anchored to the 4-K shield, which was several degrees warmer than the cryostat 4-K vessel to which it was attached.

The simulation suggested that the motion-control feedthrough tube with its internal guide assembly, the pump driveshaft and control strings, and the LHe transfer tube allowed 450 mW to 750 mW of heat into the vac-canister. This heat load is close to the amount of heat needed to account for the helium boil-off observed during data runs. Any future operation of the apparatus will include design changes that would decrease this heat load to an amount closer to the original design.

5. Experimental Control and Data Acquisition

5.1. Instrumentation

The liquid helium levels for each target chamber and the bath in the vac-canister were individually monitored with resistive-wire liquid level sensors. The temperatures on the upstream and downstream target, as well as the cryostat 4-K and 77-K vessels were monitored with silicon diode temperature sensors. The longitudinal magnetic field within the target region was measured by a fluxgate magnetometer multiplexed to four single-axis low-temperature probes. These fluxgate sensors were mounted above the targets and had a sensitivity of 0.5 nT.

5.2. Experimental Control

The control sequence for the liquid helium target system, the data acquisition, and data storage were managed by the Neutron Spin-Rotation Acquisition and Control (NSAC) program. The NSAC collected neutron beam count rates from the ionization chamber while it switched through the combinations of the two output coil rotation states ($+\pi/2$, $-\pi/2$) with the three pi-coil current states (current[-], off[0], current[+]) in a predetermined sequence. This sequence was iterated several times to build up a *target sequence* (see Figure 11).

After a target sequence was completed, the NSAC stopped collecting beam rate data, and initiated a target-change routine. The temperature sensors and one of the fluxgate magnetometer sensors were energized and allowed to warm up to operational temperature. At the same time, a motion control actuator lowered the pair of drains of the target chambers that were full of liquid helium during the preceding target sequence and allowed them to empty their liquid helium into the bath. Then, the stepper motor began spinning the centrifugal pump, which began filling all four target chambers with liquid helium from the bath.

The NSAC turned the stepper motor off after a given length of time, which allowed the pump to completely fill the pair of target chambers with the raised drains with liquid helium. Calibration testing of the centrifugal pump using varying depths

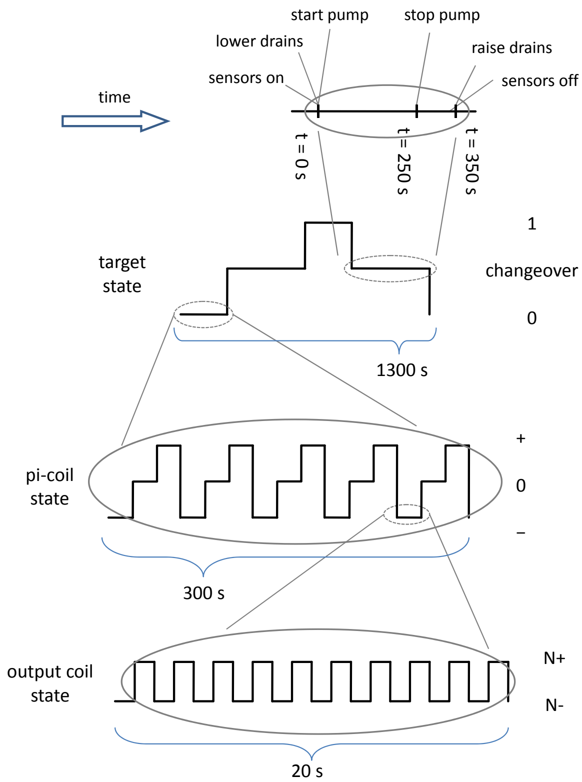

Figure 11: Diagram of the control sequence. The output coil is flipped at a rate of 1 Hz. Each pi-coil state has 10 output coil flips. Five pi-coil sequences make a target sequence. A target-change routine following each target state switched the liquid helium target between target states. Two consecutive target sequences constitute a target cycle.

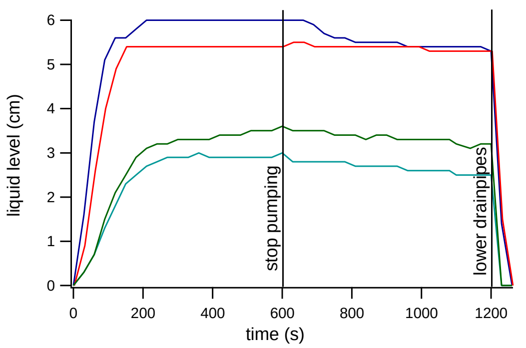

Figure 12: Plot of the liquid helium level in a target chamber as measured by a resistive wire liquid helium meter during fill and drain testing for various depths of the liquid helium bath in the vac-canister. The deepest bath depth produced the fastest fill curve, while decreases in the bath corresponded to slower fill times.

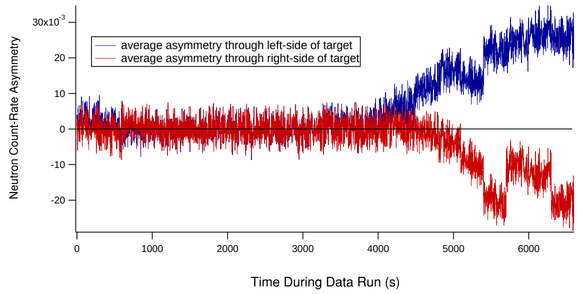

Figure 13: Plot of a run in cycle 2 where the neutron data show that the target did not fill or drain correctly during the beginning and end of the run. A large deviation from zero of the neutron count-rate asymmetry through either the left or right-side of the target indicates filling or drain problems with a target chamber.

of liquid helium in the bath indicated that stepper motor run times of 300 s was sufficient for target switch-overs that occurred in the first half of an eight-hour data run and 350 s for the later half. The difference in pump times was related to the decreasing bath depth over the duration of a run from liquid helium boil-off.

Once the centrifugal pump had stopped, data from the temperature and fluxgate sensors were recorded by the NSAC. The liquid helium was allowed to completely empty from the target chambers with lowered drains for 50 s, a time which was determined during calibration measurements. This drain time also allowed any bubbles within a full target chamber to settle out so that the liquid helium density was homogeneous during neutron data sequences. The drain time also allowed the temperature in the targets to equilibrate and any turbulence in the target chambers to subside.

After the empty target chambers drained, the actuators raised the drains and all instrumentation in the target region was powered off. The target was now in the new *target state*, and data taking could resume for the next *target sequence*. Two consecutive target sequences – one for each target state – constituted a *target cycle*. Upon completion of each target cycle, the NSAC calculated various count rate asymmetries for the target, total spin rotation angles, and parity-violating spin rotation angles ϕ_{PV} for real time analysis.

The target sequence was set to run 300 s, with 5 iterations of pi-coil and output coil states each lasting 1 second, and with the target-change routine taking either 300 s or 350 s. With the possible exception of the angular orientation of the centrifugal pump vanes and other rotating elements along the driveline, all of the locations of the moveable mechanical systems inside the target chamber are in the same location for all data runs after the liquid motion sequence.

6. Liquid Helium Target System Performance

The liquid helium target system was assembled and tested at IUCF. Basic testing of the target was conducted to ensure that instrumentation and motion control components functioned correctly at low temperatures. The apparatus was then shipped to the NCNR, and after initial beamline and polarimeter characterization studies were complete, the liquid helium target system was installed and commissioned on the NG-6 beamline.

The liquid helium target operated more or less continuously during the experiment for about six months in early 2008, executing 5406 target motion sequences with liquid helium. The target was warmed once to room temperature during a reactor shutdown to fix a small intermittent leak at the low temperature end of the G-10 tube used to repeatedly transfer liquid helium into the vac-canister. Except for this warm-up, the target was always held at a temperature no greater than 77 K to minimize the development of internal stresses on seals from differential thermal contraction.

The performance of the target fill and drain system in moving liquid between target chambers was tested prior to the experiment. Figure 12 shows the liquid helium levels as measured by the liquid level meters in the course of a fill and drain sequence similar to that used in the experiment. The data demonstrated that the centrifugal pump worked and that the drain pipes operated at designed.

During the experiment, the liquid helium levels within the target chambers could be monitored indirectly using the neutron beam transmission. The count-rate asymmetry used to calculate the neutron spin-rotation angle was separated into left and right-side target asymmetries. Any failure of the target to either fill or drain properly was indicated in the neutron data as a large deviation of these left–right target asymmetries from zero.

Figure 13 shows a plot of target asymmetries during a typical data run. The neutron data indicate that initially, the liquid helium bath was overfilled and that the drains didn't fully empty all of the chambers between target sequences. After several target sequences, normal fill and drain performance was indicated. Towards the end of the run, the neutron data indicate that the target chambers were not filling or draining properly, which coincided with the depth of the liquid helium bath decreasing below nominal operating levels due to boil-off.

The target could also be operated without liquid helium present in the target chambers or even the target chambers and vac-canister. This was done before and after the liquid helium phase of data taking to place constrains on possible systematic effects.

The temperature of the target was measured periodically throughout the run during target motion. Figure 14 shows the temperatures as measured by thermometers located at various locations on the aluminum target chamber. No evidence for excursions of the target temperature away from that expected for a liquid helium bath whose pressure is close to atmosphere was observed.

7. Conclusion

The Neutron Spin Rotation experiment acquired data from January – June 2008. The experiment is currently in the data analysis phase.

Further experiments to perform precision measurements of neutron spin rotation in liquid helium are possible using the same polarimeter and target system design. Removal of the reflective aluminum tape on the motion control feedthrough tube and

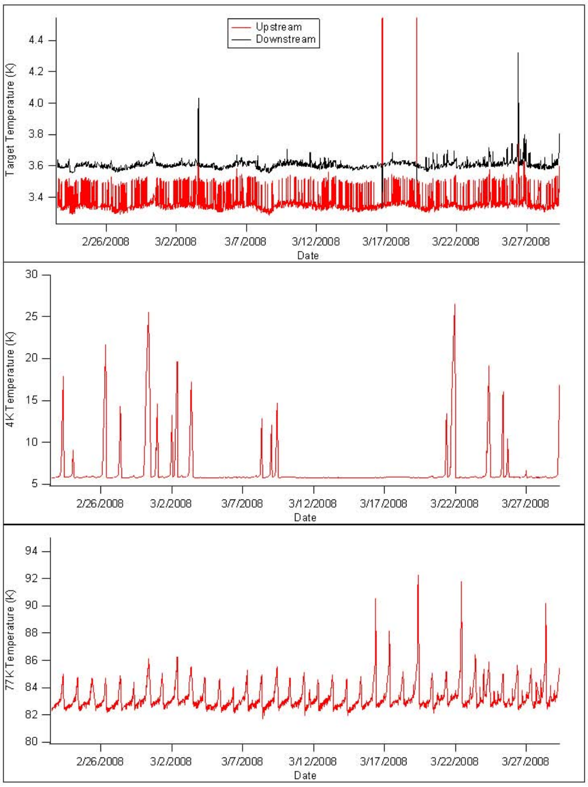

Figure 14: Plot of measured temperatures during cycle 2 of the upstream and downstream target chambers, the liquid helium jacket, and the liquid nitrogen jacket. The liquid nitrogen jacket displays daily warming and cooling that coincide with its daily fill schedule. The liquid helium jacket shows good temperature stability, with the noted exception of temperature spikes during some of the daily fills. The target temperatures similarly display temperature spikes during liquid helium fills, but at a three time per day frequency that coincided with the scheduled 8-hour runs; otherwise, the target temperatures displayed good stability during data runs.

the liquid helium transfer tube and a redesign of the thermal anchoring for these tubes should greatly reduce the liquid helium consumption rate of the target. Another improvement in target performance could come from increasing the centrifugal pump speed, thereby reducing the time needed to fill target chambers with liquid helium. This would increase the percentage of live time data-taking and so increase the available neutron count rate statistics.

In addition to measurements done with liquid helium, other targets are possible, including liquid parahydrogen [14][15][16] and liquid orthodeuterium [17][18]. These targets would require some modifications of the basic liquid helium target system for the warmer operational temperatures (20 K) as well as inclusion of hydrogen safety systems.

8. Acknowledgements

The authors acknowledge the support of the National Institute of Standards and Technology, U.S. Department of Commerce, in providing the neutron research facilities used in this work, and the support of the U.S. Department of Energy, Office of Nuclear Science and the National Science Foundation.

We thank the University of Washington for funding and use of hardware from the previous Neutron Spin Rotation experiment. We thank the Indiana University Physics Department machine shop and the University of Washington machine shop for their work on fabrication of the liquid helium target system components, and the Indiana University Cyclotron Facility for infrastructure used in the extensive target testing conducted before the experiment. We thank David Haase for his work in refurbishing the cryostat and room-temperature magnetic shielding. Christopher Bass acknowledges the support of the Ronald E. McNair Graduate Fellowship Program and the National Research Council Postdoctoral Associates Program. This work is supported in part by NSF PHY-0457219, NSF PHY-0758018, NSF PHY-9804038, and DOE DE-FG02-87ER41020.

References

[1] F. C. Michel, Phys. Rev. 133, B329 (1964).
[2] L. Stodolsky, Nucl. Phys. B 197, 213 (1982).
[3] B. Desplanques, J. F. Donoghue, and B. R. Holstein, Ann. Phys. 124, 449 (1980).
[4] M. J. Ramsey-Musolf and S. A. Page, Ann. Rev. Nucl. Part. Sci. 56, 1 (2006).
[5] C. -P. Liu, Phys. Rev. C 75, 065501 (2005).
[6] B. R. Holstein, Fizika B 14, 165 (2005).
[7] S. L. Zhu, *et al*, Nucl. Phys. A 748, 435 (2005).
[8] A. M. Micherdzinska et al., manuscript in preparation (2008).
[9] D. M. Markoff, Measurement of the parity nonconserving spin-rotation of transmitted cold neutrons through a liquid helium target, PhD Thesis, University of Washington, Seattle, 1997.
[10] C. D. Bass, Rev. Sci. Instrum. 79, 055101 (2008).
[11] V. F. Sears, Neutron News 3, No. 3, 26-37 (1992).
[12] P. M. McConnell, in NBSIR 73-316 (National Bureau of Standards, 1973).
[13] J. D. Brownridge, Cryogenics 29, 70 (1989).
[14] Y. Avishai and P. Grange, J. Phys.G: Nucl. Phys. 10, L263-L270 (1984).
[15] D. M. Markoff, J. Res. Natl. Inst. Stand. Technol. 110, 209-213 (2005).
[16] R. Schiavilla, J. Carlson, and M. Paris, Phys. Rev. C 70, 044007 (2004).
[17] Y. Avishai, Phys. Rev. Lett. 52, 1389 - 1392 (1984).
[18] R. Schiavilla et al., Phys. Rev. C 78, 014002 (2008).